COMPARISON OF VARIOUS APPROACHES TO NUMERICAL SIMULATION OF SHIP RESISTANCE AND PROPULSION

Charles Badoe (Faculty of Engineering and the Environment, University of Southampton, UK)
Björn Windén (Faculty of Engineering and the Environment, University of Southampton, UK)
Artur K. Lidtke (Faculty of Engineering and the Environment, University of Southampton, UK)
Alexander B. Phillips (Faculty of Engineering and the Environment, University of Southampton, UK)
Dominic Hudson (Faculty of Engineering and the Environment, University of Southampton, UK)
Stephen R. Turnock (Faculty of Engineering and the Environment, University of Southampton, UK)

1. SUMMARY

The prediction of a ship's wake field and its resistance and propulsion characteristics has traditionally been centered on experiments; however, with the advancement in high performance computers, this can be achieved through the use of computational methods. An advantage of using CFD is its ability to provide insight into flow characteristics close to the wall, which are difficult to obtain through experiments. The most interesting and challenging aspect of using CFD in ship resistance and propulsion analysis is the influence of the propeller action and the unsteady hydrodynamics of the rudder working in the propeller wake. One approach to address the problem is to adopt the sliding mesh approach to discretize the ship, propulsor and the rudder, (Carrica et al., 2011). This approach is the most suitable but due to the small time steps and high computational cost involved, simulations are often performed using representative propeller models or body force method. The level of complexities in the body force propeller approach varies from prescribing the body forces (Simonsen 2000), through to coupling a more complex propeller performance code which accounts for the non-uniform inflow at the propeller plane, Phillips et al., (2009). There are several computations using body force propeller models reported in the literature. Simonsen and Stern, (2003) coupled a body force propeller model based on potential theory formulation in which the propeller was represented by bound vortex sheets on the propeller disk and free vortices shed from the downstream of the propeller to a RANS code to simulate the manoeuvring characteristic of the Esso Osaka with a rudder.

Rijpkema et al., (2013) investigated the propeller-hull interaction and the determination of the effective wake field using a hybrid RANS-boundary element (BEM) approach. The coupling between the RANS and BEM was performed using an iterative coupling between the velocity fields from both RANS and BEM computations and the force distribution on the propeller blades obtained from the BEM results. The most challenging aspect of the coupling strategy was the determination of the effective wake used as input for the BEM computation. Due to the presence of singularities at collocation point of the BEM panel, the determination of velocities in the propeller plane lead to unrealistic values, hence the problem was addressed by extracting the propeller induced velocities at a plane upstream of the propeller.

The work presented in this paper compares the ability of four different methods; Hough and Ordway prescribed body force approach (i), two coupled RANS-BEMt models (ii) & (iii) and a discretized propeller approach, (iv), (hereafter referred to as methods i-iv) to capture the resistance and propulsion capabilities of a container ship with experimental data from the SIMMAN Workshop on Verification and Validation of Ship Manoeuvring Simulation Methods, (SIMMAN, 2014). For methods (i), and (ii), two simulations each were conducted; one included the effect of free surface [F] and the other utilizing a double body approach [NF]. Only one simulation was performed with method (iii) and (iv) which included the influence of freesurface [F].

The main focus here is a detailed analysis on the prediction of the hull and rudder performance resulting from the different levels of body force propeller approximations. A comparison is also made between free surface [F] and double body approach [NF] on the prediction of hull, propeller and rudder forces.

The presented study is based upon the well-known KRISO container ship (see Larsson et al., 2010), whose lines are shown in Fig. 1. The SVA hull model built and tested at Force technology was used.

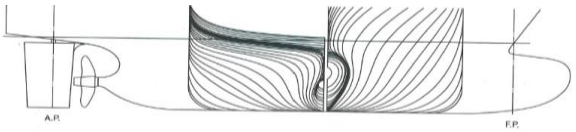

Fig. 1 Body plan and side profile of the KCS ship model, source: Fujisawa et al., (2000).

The forces and moments data for the SVA hull were obtained as part of the SIMMAN 2014 Workshop on Verification and Validation of Ship Manoeuvring Simulation Methods, (SIMMAN, 2014). Test no 2a -1 was considered. The self-propulsion test was carried out at Fn = 0.202 in the fully appended configuration and the propeller rps was set at 14. Full details of the experimental test conditions and data can be found at the SIMMAN 2014 website, (www.smmman2014.dk).

2. THEORETICAL APPROACH

2.1 RANS Formulation

The flow generated around the three propeller models, rudder and hull can be modeled by the Reynolds Averaged Navier-Stokes equations. Within the assumption of an incompressible fluid, the set of equations may be written in the form:

$$\frac{\partial \overline{U_i}}{\partial x_i} = 0 \qquad [1]$$

$$\frac{\partial \overline{U_i}}{\partial t} + \frac{\partial \overline{U_i U_j}}{\partial x_i} = -\frac{1}{\rho}\frac{\partial \overline{P}}{\partial x_i} + \frac{\partial}{\partial x_i}\left\{\nu\left(\frac{\partial \overline{U_i}}{\partial x_i} + \frac{\partial \overline{U_j}}{\partial x_i}\right)\right\} - \frac{\partial \overline{u'_i u'_j}}{\partial x_i} + \overline{f_i} \qquad [2]$$

where x_i represents the Cartesian coordinates (X, Y, Z) and U_i are the Cartesian mean velocity components ($\overline{U_x}$, $\overline{U_y}$, $\overline{U_z}$). The Reynolds stress is expressed as ($\overline{u'_i u'_j}$) and must be modeled using an appropriate turbulence model. The SST k-ω model has been successfully used for this purpose of hull-propeller-rudder interaction and wakefield analysis, (Larsson et al., 2010) making it a natural choice for the study discussed herein.

2.2 Modelling

Numerical solution of equations (1) and (2) was carried out for all methods using the open source RANS solver OpenFOAM, which is designed to solve problems in mechanics of continuous mediums; see Jasak (1996) for more details on introduction and numeric used in OpenFOAM. The RANS equations were solved using a cell centered finite volume method (FVM). Discretization of the convection terms was achieved using Gauss linear second order upwind and the diffusion terms were treated using the central difference scheme. The SIMPLE algorithm was used for the pressure-velocity coupling. In the case of the free-surface flow computations, the PIMPLE algorithm was used for pressure-velocity coupling and a vanLeer scheme with interface compression was used for the VOF and volume fraction discretization respectively. The pressure correction equation was under relaxed with a factor of 0.3, which was found as a compromise between stability and convergence speed. In method (iv), first-order schemes were applied to the turbulent quantities, the convection term was discretized using a first-second order approach. First order Euler time-stepping scheme was utilized in conjunction with the PIMPLE algorithm to advance the unsteady solution. Two outer loops, each with two inner pressure loops, were run until the residuals converged to at least 1e-8 at each time step.

The simulation was initialized from a steady-state naked hull solution and then ran for approximately 10 propeller revolutions. The fields were averaged by employing a script which loops over the time directories, reads the field and then writes the averaged field for any user specified time requirement.

2.3 Hough and Ordway prescribed body force approach and coupling methodology (method i)

In this approach the impact of the propeller on the fluid is represented as a series of axial and tangential momentum sources. Their strength is then calculated using the Hough and Ordway thrust and torque distribution, (Hough and Ordway, 1965). This closely matches the optimum distribution, Goldstein, (1929). It has been used by others such as Simonsen, (2000) and Phillips et al., (2009) to replicate the action of the propeller in several marine applications. A complete description of the methodology can be found in Badoe et al., (2012).

2.4 BEMt propeller model and coupling methodology (method ii)

An existing BEMt code (Molland and Turnock, 1996) was modified and coupled to a RANS solver (the same solver as 2.2), whereby within the RANS mesh the propeller is represented as a cylindrical domain with diameter equal to that of the propeller diameter, D and a length of 0.1D. The propeller is adapted to the hull wake by employing a sectorial approach where the propeller domain is sub divided into a series of nC circumferential, and nR radial slices along the blade. An example of a BEMt mesh is presented in Fig. 2. A complete description of the methodology can be found in Badoe et al., (2014).

The simpleFoam solver, a steady state solver for incompressible, turbulent flows and the LTSInterfoam solver, a local time stepping solver for two incompressible, isothermal immiscible fluid using the VOF phase-fraction based interface capturing approached in OpenFOAM were modified to accommodate the coupling for the double body and free surface simulations respectively.

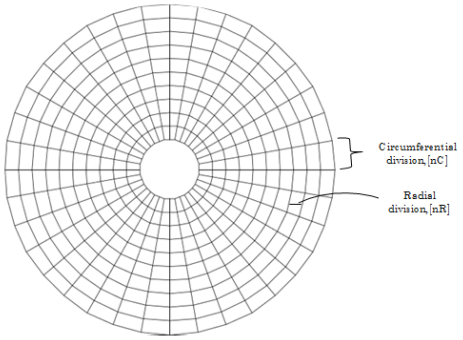

Fig. 2 BEMt propeller mesh showing radial, nR, and circumferential, nC, subdivisions.

2.5 BEMt propeller model and coupling methodology (method iii)

A coupled RANS-BEMt solver is created using the method described by Windén (2014). This as further discussed by Windén., (2013) presents the use of a modular framework for coupling a FV flow solver on an arbitrary mesh with an arbitrary body force model for the propeller. Here, the BEMt equations are solved on a separate structured concentric mesh with the background FV mesh being adapted to best fit around the hull. Interpolation from the FV mesh to the concentric mesh is conducted to obtain the propeller inflow and vice versa to obtain the body force distribution for the solution of the momentum equation.

Due to discrepancies in the assumptions in the derivation of the RANS equations and those of the BEMt theories used and due to the lack of detail in the propeller model, the theoretical propeller induced velocities are not well matched with those obtained from probing the RANS solution (Windén 2014). To compensate for this, Windén (2014) created an ad hoc correction which is valid for a particular propeller geometry. The axial inflow velocity "far upstream", i.e. with the propeller induced velocities subtracted is calculated as

$$U_1 = \frac{U_2}{U_\infty(1+a_\infty)} - (\psi_{lin} + \psi_{triq}) + U_\infty \qquad [3]$$

where a_∞ is the axial inflow factor.

Equation [3] is corrected for a finite number of blades using

$$a_\infty = \sqrt{\frac{1}{4} + Ka(1+a)} - \frac{1}{2} \quad [4]$$

and

$$\psi_{lin} = 1.6790 - 1.3744J + 0.7424J^2 + \frac{r}{R}(-0.7606 + 1.3864J - 0.6705J^2) \quad [5]$$

$$\psi_{triq} = J^{-2.7048}\left(0.7370\left(\frac{r}{R} - 0.5587\right)^5 + 0.0694\left(\frac{r}{R} - 0.5582\right)^3\right) \quad [6]$$

where *a* is the axial inflow factor from the converged blade element solution, *K* is the Goldstein correction factor and *r/R* is the relative location along the blade.

This correction allows for the propeller induced velocities to be separated from the total wake at run-time. This in turn allows the model to find a balance between the thrust and the ships resistance in a single run without the need for an iterative procedure as in methods (i) and (ii). It also allows for the wake to be unsteady and the resulting fluctuations of thrust and torque to be studied.

The simulation is run in two steps. First the steady wave pattern is allowed to develop. When the calm water resistance is found, the propeller model is activated and the simulation is run until the resistance, thrust and torque reach steady values. Note that only one simulation is necessary per mesh. With run-time removal of the propeller induced velocities, there is no need to stop the simulation and update the nominal wake as carried out in methods (i) and (ii).

2.6. Discretized propeller approach (method iv)

The discretized propeller approach employs a sliding grid provided by the arbitrary mesh interface (AMI) for non-conformal mesh regions. This technique allows flow data to be exchanged across disconnected mesh domains which can either be stationary or moving relative to one another. In the discussed context, it operates by projecting one of the sides of the interface on to the other and is used for handling rotating meshes. The AMI idea is based on a set of weighting factors that balances the fluxes at the region interface. An example of the AMI interface for a propeller is shown in Fig. 3. The drawback to this approach is that it is computationally much expensive since the full transient flow field needs to be resolved. Moreover the cell count required also increases as the fine detail of the propeller needs to be resolved. This becomes particularly limiting as one considers the difference of the significant flow feature scales for the hull and propeller.

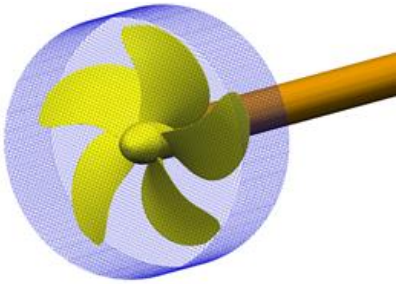

Fig. 3 Example of an AMI interface for the KCS propeller in open-water.

3. GRID GENERATION

Unstructured, predominantly hexahedral grids with local refinements around no slip walls were used in the study. All grids were created using blockMesh and snappyHexMesh utilities forming part of the OpenFOAM libraries. The grids were congregated in the regions of the stern, bow, near the hull surface and the free surface. Ten to twelve elements were used to capture the boundary layer of the hull and rudder yielding an approximate y^+ of 60 for the hull and 30 for the rudder. The total number of grids used was approximately 8million for methods (i) and (ii) and 18 million for method (iii). For method (iv) a mesh of 12.7 million cells was used to conduct the sliding mesh interface computation, with 4 million used to discretise the propeller and the rest placed in the vicinity of the hull and rudder. Fig. 4 shows the mesh resolution for the stern for methods (iv) and (i & ii) respectively.

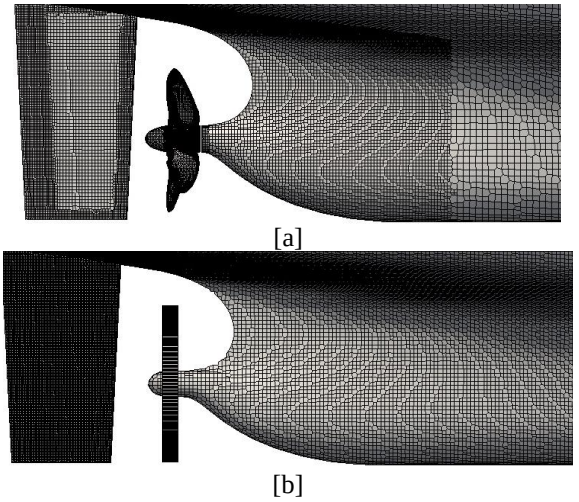

[a]

[b]

Fig. 4 KCS stern mesh; method (iv) shown in [a] and methods (i) & (ii) depicted in [b].

4.1. Grid sensitivity

A sensitivity analysis has been carried out using method (iii) with the inflow correction to find the resistance and propulsion characteristics of KCS. Three meshes shown in Table 1 are used. The BEMt grid size of 10x10x1 elements was used for all cases. The table also shows the size of the concentric mesh used to perform the BEMt calculations, how many FV cells are inside the propeller disk and how much of the total clock time is spent on propeller modelling. This percentage includes mapping, data handling as well as solving the specific equations. The predicted total resistance as seen from Table 2 is within 5% of data on all grids. In all parameters variations from one grid to another was monotonic.

Table 1 Grid system used for sensitivity analysis, Method (iii).

Grid	Grid size	Cells in propeller disc	BEMt computational expense
Fine	17.7M	3500	2.4
Medium	10.8M	2600	1.6
Coarse	3.1M	400	1.0

Table 2. Grid convergence study for the KCS at Fn=0.202, rps =14, Method (iii).

Parameter	Grid Coarse	Medium	Fine	Data
$1000C_T$	5.0898	5.1540	5.563	5.318
ε	4.30%	3.08%	4.61%	
K_T	0.2620	0.2808	0.2810	0.302
ε	13.25%	7.02%	6.95%	
K_Q	0.0425	0.0460	0.0461	0.0429
ε	0.93%	7.23%	7.46%	

ε = %Data

4. RESULTS

4.1. Propeller open water prediction

The open-water performance shown in Fig. 5 calculated from the BEMt propeller code (in method ii) and AMI (method iv) is compared with values from SVA. The trend in K_T plots highlights the good agreement of the predicted thrust of the propeller for both methods. For the effective advance speed of interest for this work (nominal J=0.6) the agreement for K_T and 10 K_Q was excellent for method (ii), with difference of less than 0.2% whilst that of method (iv) showed differences of 9%. The large variation in method (iv) is attributed to insufficient mesh resolution around the blades and its boundary layer.

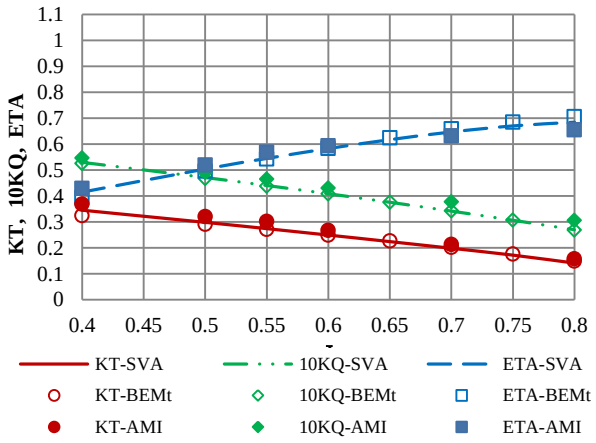

Fig. 5 Comparison of propeller characteristics in open water. Experimental data made available as part of the SIMMAN 2014 workshop, (SIMMAN, 2014).

4.2. Resistance and propulsion characteristics

Axial velocity distributions along various locations on the hull were taken to compare the strengths and weaknesses of all methods in predicting the stern flow. Fig. 6, shows one such plot for 0.9 propeller diameters upstream of the propeller plane with running propeller and a double body approach [NF]. No significant differences can be observed for all methods used. All methods predicted almost the same hull boundary layer size. As the flow approaches the propeller the differences in the various methods becomes clear (Fig. 7.). Method (i) shows symmetry in the flow as it tries to replicate the swirl effect. This is because the method assumes a constant circumferential distribution of thrust and torque whilst it is actually not true in reality. Method (ii) is more consistent with method (iv), which shows the actual propeller hydrodynamic influence on the inflow and as such a different flow regime to that of method (i) can be seen. The differences results from the sectorial approach adopted for the propeller which unlike method (i) does not use an average circumferential distribution but rather takes into account the local thrust and torque at each radial and circumferential location in the propeller plane. This results in an asymmetry in the flow field. The load on the port side of the propeller in method (ii) is much greater compared to method (iv). Since no experimental flow field data was provided, an in depth flow field comparison between these two method proved difficult however it should be borne in mind that a 9% increase in propeller force for J=0.6 was achieved with method (iv) with the level of mesh density used as such might contribute to the reason for the differences in plots.

Table 3 shows a combined results for resistance and propulsion parameters for all methods with [F]and without [NF] the influence of free surface effect. By taken the free surface account method (ii) was superior in predicting the resistance and thrust by less than +5% of the experimental data with method (iii) showing values less than 18%. Although a prescribed thrust and torque value was used in method (i) the resistance was predicted within +23%. The swirl effect induced by the BEMt propeller in flow using method (iii) was much better with differences of +7%D compared to +15%D of method (ii).

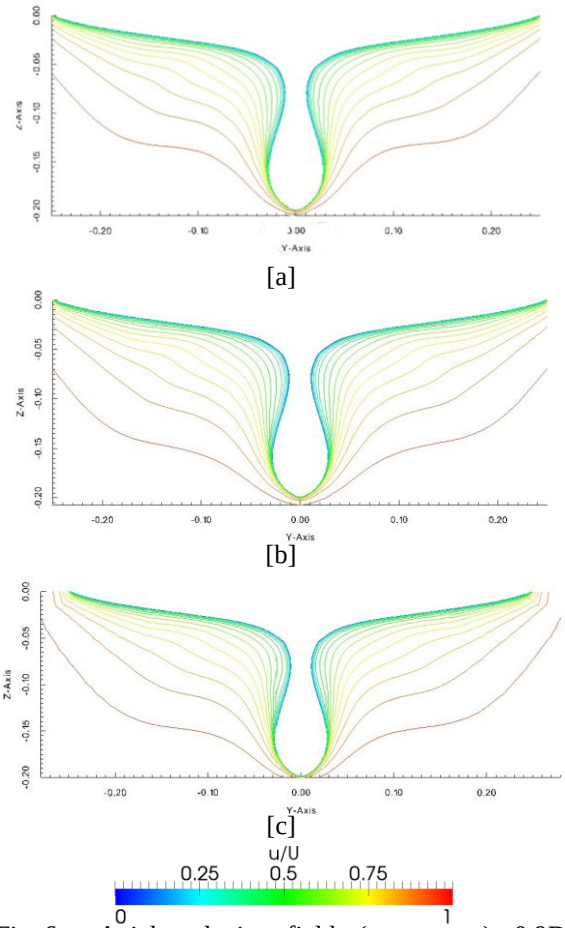

Fig. 6 Axial velocity field (u contour) 0.9D upstream of propeller plane, Fr 0.202 from [a] method (i, NF) [b] method (ii, NF) and [c] method (iv, NF) at n_p = 14.0rps.

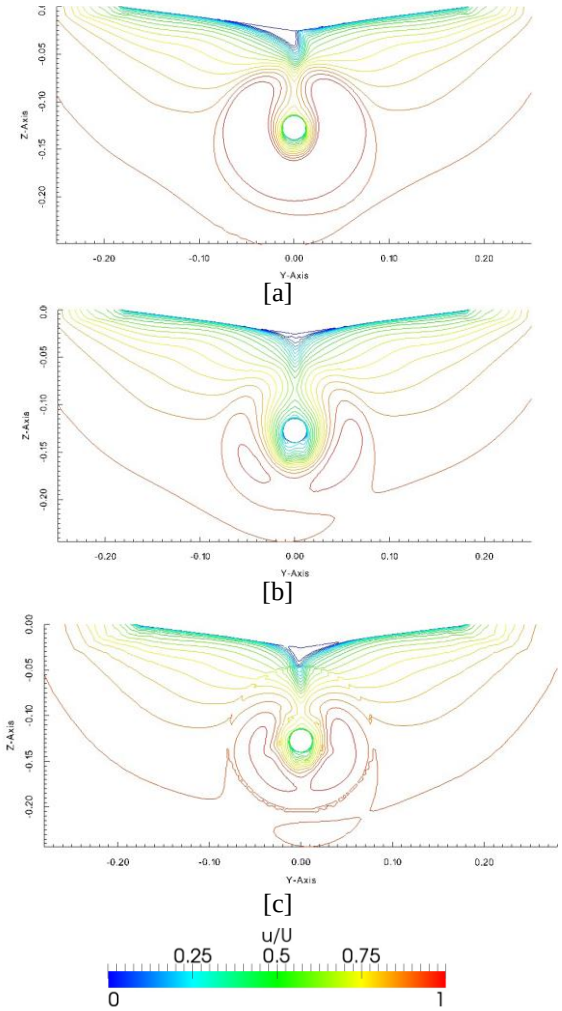

Fig. 7 Axial velocity field (u contour) 0.1D upstream of propeller plane, Fr 0.202 from [a] method (i, NF) [b] method (ii, NF) and [c] method (iv, NF) at n_p = 14.0rps.

Resistance and propulsion results using the double body approach [NF] shows a +5%, +19% and -3% prediction in thrust, torque and resistance respectively using method (ii) compared to -17%, -16% and -23% of method (iv). The high values of method (iv) was expected since the propeller open-water data was over predicted. It should be noted however that the hull-propeller-rudder forces are dependent on how accurate each of these component is predicted. An increased or decreased in prediction of one will travel down the chain resulting in increased or decrease in prediction in the others.

Method (ii) shows that at Froude number, Fn=0.202, the differences in thrust and torque increases by approximately 4% when a double body approach is used and the resistance decreases by 7%.

The downstream rudder forces in the x-direction were low for methods (ii and iv) whilst that of (i, ii and iv) was high in the y-direction. No experimental data was provided for the rudder forces, however it should be noted that rudder forces are dependent on the inflow conditions (hull wake and propeller race) which in turn are dominated by the action of the propeller, slight over or under prediction in propeller force will caused an increased or decreased inflow velocity to the rudder, causing an increase or decrease in rudder forces.

Table 3: Resistance and propulsion parameters.

Parameter $\times 10^{-4}$	Method (i)	Method (ii)	Method (iii)	Method (iv)	Data
	F/NF	F/NF	NF	NF	
X'	141.7/168.5	192.2/179	150.8	141.3	184.2
Y'	19.35/14.62	10.32/17.1	2.960	18.24	-0.64
N'	-9.73/-7.08	-4.0/-5.60	-1.10	-8.96	-2.80
$R_X{}'$	15.04/17.38	4.66/6.84	16.23	5.21	-
$R_Y{}'$	18.96/8.52	7.43/14.85	2.70	16.79	-
T'	P/P	390/403	358.2	319.7	386.2
Y'	P/P	2.16/2.24	2.010	1.570	1.880

Note: X'-hydrodynamic longitudinal force; N'-hydrodynamic yaw moment; Rx'-rudder force in x direction; Ry'-rudder force in the y direction; T'-propeller thrust; Q'-propeller torque; P-prescribed thrust and torque (open-water data values), NF: - Double body approach, F: - Freesurace surface included.

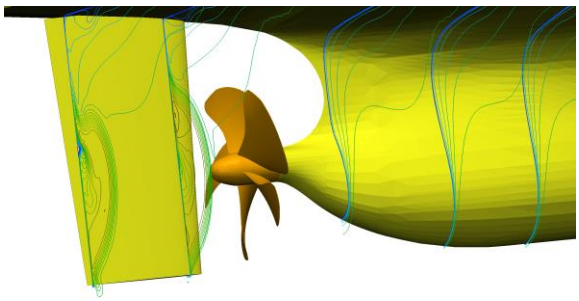

Fig. 8 Instantaneous velocity profiles for the stern region obtained using method (iv).

Fig. 8 presents instantaneous boundary layer profiles for the stern region obtained using the AMI (interface (method (iv)). One may clearly see the evolution of the velocity deficit at the propeller inflow caused by the hull boundary layer. It is also interesting to note how the accelerated flow impinges on the rudder. This is further affected by the interaction of the blade tip vortex with the rudder surface.

5. CONCLUSIONS

In summary the flow around the KCS container ship with and without rudder has been calculated using four different methods to gain insight into the flow field and resistance and propulsive characteristics of the ship model. The predicted forces compared reasonably well with experimental results for all methods with the level of mesh density used even though method (iv) would have benefitted with a much finer mesh around the propeller blades and in the boundary layer.

By using a double body, the thrust and drag increased by 4% and resistance decrease by 7% using method (ii) for Froude number of Fn=0.202. Accounting for the free surface effect is time consuming and computationally demanding since smaller time steps and long runs are needed for the waves to settle before extracting the inflow velocities for the propeller and since the results are within the likely bounds of experimental error, an alternate and quicker option of predicting the resistance and propulsion parameters will be to run the simulation without the free surface and then use a linear potential flow code to predict the wave resistance. This however should only be applicable for Fn $\leq$ 0.202.

Method (i) assumes a constant circumferential distribution of thrust and torque hence does not capture the interaction between the hull on propeller and rudder on propeller and vice versa. The method estimated the resistance with reasonable accuracy, but was poor in replicating the swirl effect which resulted in a different flow field (i.e. symmetry in the flow field) compared to the other methods. This method can be used for quick resistance and self-propulsion estimations only if the flow field details are not of prime importance as long as the required conditions of the flow heads are captured.

Methods ii, (and also iii and iv) is best suited for capturing and predicting most aspect of the resistance and propulsion characteristics of a ship. The method calculates the thrust and torque as part of the simulation and able to give estimates of the interaction between the hull on propeller and rudder on propeller. It is able to replicate the swirl effect much better than method (i) and results in a significantly lower in computational cost compared to method (iv) for resistance and self-propulsion simulation. The drawback of this method is that it is much slower than method (iii) in finding the self-propulsion point, because it uses the conventional approach of starting and stopping the simulation and updating the rpm until the self-propulsion point is reached however the order of accuracy is much better.

Method (iii) showed a -7%, +7% and -18% of experimental data for thrust, torque and straight line resistance compared to +1%, +15% and +4% for method (ii). This is reasonably good considering that the forces are achieved with no extra treatment of the FV mesh with regards to the propeller model and with only a few extra per cent of extra computational time compared to a standard calm water resistance and self-propulsion prediction as in methods (i, ii and iv). This is encouraging for the use of this approach for self-propulsion simulations. While this simulation is steady, the run-time treatment of the wake allows for unsteady simulations to be conducted.

Method (iv) is the most computationally expensive approach since the full transient flow field needs to be resolved with a higher level of mesh cells in order to provide accurate estimates of resistance and propulsion parameters.

REFERENCES

Badoe, C., Phillips, A.B. and Turnock, S.R., (2012), Initial numerical propeller rudder interaction studies to assist fuel efficient shipping, in 'Proceedings of the 15th Numerical Towing Tank Symposium, 7-9 October, Cortona Italy'.

Badoe, C., Phillips, A.B. and Turnock, S.R., (2014), Ship wake field analysis using a coupled BEMt-RANS approach, in 'Proceedings of the 17th Numerical Towing Tank Symposium, 28-30 September, Marstrand Sweden'.

Carrica, P.M., Alejandro, M., and Stern, F., 2011. Full scale self-propulsion computations using a discretized propeller for the KRISO container ship KCS. Journal of computers and fluids marine science and technology, 51, pp.35-47.

Fujisawa, J., Ukon, Y., Kume, K., and Takeshi, H., 2000. Local velocity measurements around the KCS Model (SRI M.S. No. 631) in the SRI 400m Towing Tank, Ship Perf. Div. Rep. No. 00-003-2, SRI, Tokyo, Japan.

Goldstein, S., 1929. On the Vortex Theory of Screw Propellers. Proc. of the Royal Society, 123, 440, (A).

Hough, G.R. and Ordway, D.E., (1965), The generalized actuator disc. Developments in theoretical and applied mechanics, 2, 317-336.

Larsson, L., and Zou, L., 2010. CFD prediction of local flow around the KVLCC2 tanker in fixed condition. A Workshop on Numerical Ship Hydrodynamics: The Gothenburg 2010 Workshop December 8-10, 2010.

Molland, A.F., and Turnock, S.R., 1996. A compact computational method for predicting forces on a rudder in a propeller slipstream. Transactions of the Royal Institution of Naval Architects, 138, pp.227–244.

Phillips, A.B., Turnock, S.R. and Furlong, M.E., (2009), Evaluation of manoeuvring coefficients of a self-propelled ship using a blade element momentum propeller model coupled to a Reynolds averaged Navier-Stokes flow solver. Journal of ocean engineering, 36(15-16), pp.1217-1225.

Phillips, A.B., Turnock, S.R. and Furlong, M.E., (2010), Accurate capture of rudder-propeller interaction using a coupled blade element momentum-RANS approach. Journal of Ship Technology Research, 57(2), pp.128–139.

Rijpkema, D., Starke, B and Bosschers, J., (2013), Numerical simulation of propeller-hull interaction and the determination of the effective wake field using a hybrid RANS-BEM approach, in 'Proceedings of the Third International Symposium on Marine Propulsors, Tasmania, Australia'.

SIMMAN., (2014). Workshop on verification and validation of ship manoeuvring simulation methods. Assessed April 2014, from www.simman2014.dk/cms/site.aspx?p=13307.

Simonsen, C. (2000), Propeller – rudder interaction by RANS. PhD Thesis, Department of Naval Architecture and Offshore Engineering, University of Denmark.

Simonsen, C., and Stern, F., (2003), Verification and Validation of RANS manoeuvring simulation of Esso Osaka: effects of drift and rudder angle on forces and moments. Journal of Computers and Fluids, 32, pp.1325-1356.

Windén, B., Badoe, C., Turnock, S., Phillips, A. and Hudson, D. (2013), Self-propulsion in waves using a coupled RANS-BEMt model and active RPM control, in 'Proceedings of the 16th Numerical Towing Tank Symposium, 2-4 September, Duisburg Germany'.

Windén, B. (2014), Powering Performance of a Self-Propelled Ship in Waves, Ph.D. Thesis, University of Southampton